

Inner-Heliosphere Signatures of Ion-Scale Dissipation and Nonlinear Interaction

Trevor A. Bowen,^{1,*} Alfred Mallet,¹ Stuart D. Bale,^{1,2,3,4} J. W. Bonnell,¹ Anthony W. Case,⁵ Benjamin D. G. Chandran,^{6,7} Alexandros Chasapis,⁸ Christopher H. K. Chen,⁴ Die Duan,^{1,9} Thierry Dudok de Wit,¹⁰ Keith Goetz,¹¹ Jasper S. Halekas,¹² Peter R. Harvey,¹ J. C. Kasper,^{13,5} Kelly E. Korreck,⁵ Davin Larson,¹ Roberto Livi,¹ Robert J. MacDowall,¹⁴ David M. Malaspina,⁸ Marc Pulupa,¹ Michael Stevens,⁵ and Phyllis Whittlesey¹

¹*Space Sciences Laboratory, University of California, Berkeley, CA 94720-7450, USA*

²*Physics Department, University of California, Berkeley, CA 94720-7300, USA*

³*The Blackett Laboratory, Imperial College London, London, SW7 2AZ, UK*

⁴*School of Physics and Astronomy, Queen Mary University of London, London E1 4NS, UK*

⁵*Smithsonian Astrophysical Observatory, Cambridge, MA 02138 USA*

⁶*Department of Physics & Astronomy, University of New Hampshire, Durham, NH 03824, USA*

⁷*Space Science Center, University of New Hampshire, Durham, NH 03824, USA*

⁸*Laboratory for Atmospheric and Space Physics, University of Colorado, Boulder, CO 80303, USA*

⁹*School of Earth and Space Sciences, Peking University, Beijing, 100871, China*

¹⁰*LPC2E, CNRS and University of Orléans, Orléans, France*

¹¹*School of Physics and Astronomy, University of Minnesota, Minneapolis, MN 55455, USA*

¹²*Department of Physics and Astronomy, University of Iowa, Iowa City, IA 52242, USA*

¹³*Climate and Space Sciences and Engineering, University of Michigan, Ann Arbor, MI 48109, USA*

¹⁴*Solar System Exploration Division, NASA/Goddard Space Flight Center, Greenbelt, MD, 20771*

We perform a statistical study of the turbulent power spectrum at inertial and kinetic scales observed during the first perihelion encounter of Parker Solar Probe. We find that often there is an extremely steep scaling range of the power spectrum just above the ion-kinetic scales, similar to prior observations at 1 AU, with a power-law index of around -4 . Based on our measurements, we demonstrate that either a significant ($> 50\%$) fraction of the total turbulent energy flux is dissipated in this range of scales, or the characteristic nonlinear interaction time of the turbulence decreases dramatically from the expectation based solely on the dispersive nature of nonlinearly interacting kinetic Alfvén waves.

RCSm

Introduction.— In many astrophysical settings, the background plasma is both highly turbulent and nearly collisionless. The dissipation of this collisionless turbulence is important for heating the plasma [1–6], but the precise physical mechanisms involved are still a matter of debate [7]. As an example, the observed ion temperature profiles in the solar wind requires significant (perpendicular) ion heating, which is likely initiated at around the ion scales where particles can interact efficiently with electromagnetic waves [8]. Such heating should cause a transfer of energy from the waves to the particles around the ion scales, and thus would cause a steepening of the spectrum at these scales; this motivates our present study.

The solar wind provides a convenient example of collisionless plasma turbulence that can be studied using *in situ* spacecraft observations. Taylor’s hypothesis $\omega_{nl} \ll k_{\perp} V_{\text{SW}}$, where V_{SW} is the solar wind speed, is assumed to be well satisfied, so that the observed spacecraft-frame frequency spectra may be simply converted to wavenumber spectra. At large scales (much larger than characteristic ion-kinetic scales), the dominant turbulent fluctuations appear to be nonlinearly-interacting Alfvénic turbulence [9], with a power-law spectrum between $k_{\perp}^{-5/3}$ [10] and $k_{\perp}^{-3/2}$ [6, 11], in rough agreement with various MHD turbulence theories [12–15]. At scales much smaller than the ion gyroradius

$\rho_i = v_{thi}/\Omega_i$ (with $v_{thi} = \sqrt{2T_{0i}/m_i}$ the ion thermal speed and $\Omega_i = ZeB_0/m_i$ the ion gyrofrequency), the spectrum steepens to about $k_{\perp}^{-2.8}$ [16–18], as the non-dispersive Alfvénic turbulence transition to dispersive kinetic Alfvénic turbulence, as confirmed, for example, by measurements of the density fluctuation spectrum [19]. This steepening occurs due to the change in the dispersion relation, and occurs even without any dissipation: a fluid approximation to the dynamics in this range of scales (ERMHD) leads to a prediction of an $k_{\perp}^{-7/3}$ spectrum [20], while simulations of this fluid approximation obtain a $k_{\perp}^{-8/3}$ spectrum [21], which has been ascribed to intermittency. Our results will broadly confirm this picture of the large- and small- scale turbulent spectrum.

In addition to these power-law scalings at large and small scales, a “transition range” around the ion scales with a spectrum significantly steeper than the $k_{\perp}^{-2.8}$ in the sub-ion range has often been observed in the solar wind [22–27]. Because this anomalous steepening disappears at scales deeper in the sub-ion range, it is not possible to explain by means of the kinetic Alfvén wave (KAW) dispersion relation. The two main proposed explanations are, first, strong dissipation of the turbulence around the ion scales [28], and, second, nonlinear effects which may increase the characteristic cascade rate of the turbulence: e.g., the onset of reconnection [29–31], the

increasing importance of nonlinear interactions between co-propagating waves [32], or the influence of coherent structures [27, 33, 34]. In this Letter, we assess these two possibilities using a simple model which is agnostic as to the exact physical mechanisms responsible for dissipation and increased cascade rates.

Cascade model.— We use a Batchelor cascade model [35, 36]. The turbulent energy flux ϵ_{k_\perp} through wavenumber k_\perp is related to the spectrum $E_{k_\perp} = b_{k_\perp}^2/k_\perp$, b_{k_\perp} being the turbulent amplitude at k_\perp , via

$$\epsilon_{k_\perp} = \omega_{nl} k_\perp E_{k_\perp}, \quad (1)$$

where

$$\omega_{nl} = k_\perp b_{k_\perp} \tilde{\omega}_{k_\perp} = k_\perp^{3/2} E_{k_\perp}^{1/2} \tilde{\omega}_{k_\perp} \quad (2)$$

is the characteristic nonlinear frequency [58] (inverse cascade time) at k_\perp , and $\tilde{\omega}_{k_\perp}$ parametrizes both dispersive (e.g., from the dispersive KAW [20]) and/or nonlinear effects (e.g. caused by dynamic alignment [13], intermittency [21], or reconnection [29]). In statistical steady state far from the injection scales (cf. [36, 37]) one obtains a simple equation with solution

$$1 - \hat{Q}_{k_1, k_2} = \frac{\epsilon_{k_2}}{\epsilon_{k_1}} = \exp \left\{ - \int_{k_1}^{k_2} \frac{\gamma_{k_\perp}}{\omega_{nl}} \frac{dk_\perp}{k_\perp} \right\}, \quad (3)$$

where γ_{k_\perp} is the energy dissipation rate at k_\perp (we do not specify a physical mechanism), and \hat{Q}_{k_1, k_2} is the fractional heating rate over the range $[k_1, k_2]$. If $\gamma_{k_\perp} = 0 \forall k_\perp \in [k_1, k_2]$, then ϵ_{k_\perp} is conserved between k_1 and k_2 . Using Eqs. 1-2,

$$\frac{E_{k_2}}{E_{k_1}} = \left(\frac{k_2}{k_1} \right)^{-5/3} \left(\frac{\epsilon_{k_2}}{\epsilon_{k_1}} \right)^{2/3} \left(\frac{\tilde{\omega}_{k_1}}{\tilde{\omega}_{k_2}} \right)^{2/3}. \quad (4)$$

Deviations from a $k^{-5/3}$ spectrum (first bracket) must be caused by either dissipation (second bracket) or dispersive/nonlinear effects (third bracket) [59]. In our analysis, we use Eq. 4 to relate *in situ* measurements of the spectrum to estimates of the heating rate and/or anomalous $\tilde{\omega}_{k_\perp}$ scalings in the transition range.

Data and fitting.— The FIELDS [38] and Solar Wind Electron Alpha and Proton (SWEAP, [39]) instrument suites on the Parker Solar Probe (PSP) mission [40] provide *in situ* measurements of the inner-heliosphere plasma environment, enabling detailed studies of turbulence [6, 41, 42]. Preliminary observations using MAG data show a steep f^{-3} to f^{-4} spectrum of the magnetic field fluctuations close to the ion scales [43–45], but the noise floor of the MAG at higher frequencies has so far precluded a detailed study.

In this Letter, we use a data-set which merges the PSP/FIELDS MAG and SCM measurements [46], operating at 293 samples per second, enabling simultaneous measurements of the full range of inertial, transition, and

kinetic turbulent scales. Our data is from the first PSP perihelion encounter, when the spacecraft was magnetically connected to a small equatorial coronal hole generating slow, but highly Alfvénic solar wind [43], from 2018-11-04/09:28:19 to 2018-11-07/09:28:19. We separate the encounter into intervals of 2^{16} samples (~ 223.69 s). A 50% overlap between intervals is used to improve statistics. Average plasma n_0 , T_{0i} , and T_{0e} are computed for each interval using the SWEAP data [39, 47, 48]. The spectral density is computed by averaging eight non-overlapping sub-intervals of vector magnetic field measurements. Intervals were rejected if no finite SWEAP measurements exist, or if the SCM was in a low gain mode (~ 1 hr each day). Intervals with ion scale waves, observable in 30–50% of radial field intervals, which strongly affect measurements of ion-scale turbulence, are excluded [43, 49]. In total, 227 intervals were kept. We consider frequencies up to 100 Hz, corresponding to $k_\perp \rho_i \approx 10$, avoiding the SCM noise floor which is occasionally reached at higher frequencies.

KAW have intrinsic density fluctuations [20, 50], which at $k_\perp \rho_i \gtrsim 1$ provide a non-negligible contribution to the total free energy. We estimate this contribution by determining δn_e from the pressure balance $\delta B_\parallel / B_0 = -(\beta_i/2)(1 + ZT_{0e}/T_{0i})\delta n_e/n_{0e}$, appropriate for KAW, and estimate the total free energy [60] as

$$E_{\text{tot}} = \frac{|\delta \mathbf{B}|^2}{2\mu_0} + \frac{n_{0e} T_{0e}}{2} \left(\frac{\delta n_e}{n_0} \right)^2. \quad (5)$$

Figure 1(a) shows an example interval with transition-range steepening to an approximate f^{-4} spectrum at ion scales, similar to Cluster observations at 1 AU [25, 26]. At the highest frequencies, the measured spectral index is consistent with the modified kinetic Alfvén wave scaling of $E \propto f^{-8/3}$. Anomalous transition-range steepening is not present in a second example interval, presented in Figure 1(b), but an approximate $f^{-8/3}$ scaling at the higher frequencies is evident.

Spectra are fit with two-power-law (2PL) and three-power-law (3PL) functions using non-linear least square optimization of χ^2 residuals. Figure 1 shows the local moving window spectral index computed over a decade of frequencies for the data and each model (Figure 1(c,d)). The 3PL fit allows for determination of spectral indices of the inertial (α_I), transition, (α_T), and kinetic (α_K) ranges and the break points (f_{IT}^* and f_{TK}^*). The inclusion of a third spectral range introduces two additional degrees of freedom (the transition break, f_{IT}^* , and index, α_T), which inherently improve the square residuals [61]. The significance of the improvement in χ_{3PL}^2 (over χ_{2PL}^2) when removing degrees of freedom (DOF), e.g. through including more fit parameters, is determined by the probability $P(F)$ of drawing F from the appropriate

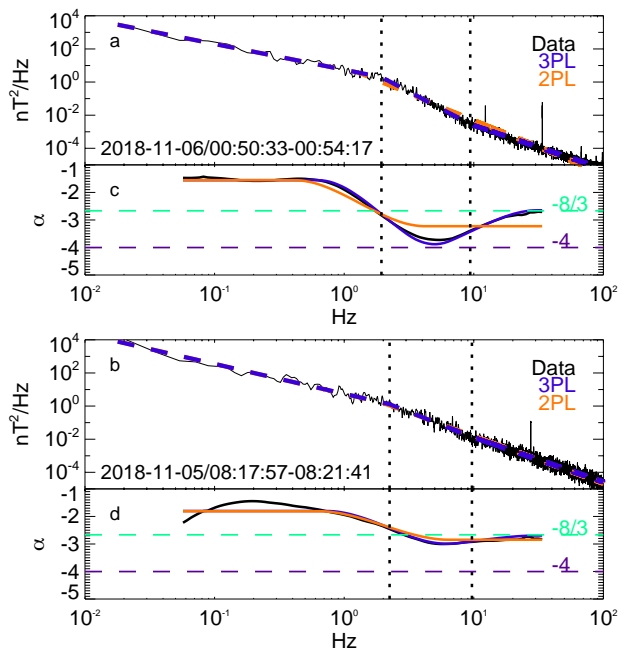


FIG. 1: (a,b) Examples of PSP/FIELDS magnetic field spectra with 3PL (blue) and 2PL fits (orange). Black dashed lines show measured 3PL spectral breaks. (c,d) spectral indices computed from data (black), 3PL (blue) and 2PL fits (orange). Dashed lines are shown corresponding to spectral indices of $-8/3$ (teal) and -4 (purple). Top interval has statistically significant spectral steepening, while the bottom interval is well modeled by the 2PL fit.

f -distribution [51]:

$$F = \frac{\chi_{2PL}^2 - \chi_{3PL}^2}{DOF_{2PL} - DOF_{3PL}} / \frac{\chi_{3PL}^2}{DOF_{3PL}}.$$

Figure 2(a) shows the distribution of measured f -test significance values, $P(F)$. The continuum of significance values suggests that transition range steepening is possibly caused by some continuously-variable, non-universal process. We separate the distribution into populations corresponding to the bottom and top half percentiles, approximately distinguishing intervals best fit by 3PL from intervals for which the 2PL fit is sufficient. The notation χ_{3PL}^2 and χ_{2PL}^2 refers respectively to the two populations.

Figure 2(b) shows the histogram of measured spectral indices for 3PL fits for α_I , α_T , and α_K . Distributions are shown separately for χ_{2PL}^2 and χ_{3PL}^2 . For the χ_{3PL}^2 population, the spectral index for the transition range has a mean of $\langle \alpha_T^{\chi_{3PL}^2} \rangle = -3.9$, standard deviation of 0.42, and range of $[-5.8, -3.1]$. Table I shows mean spectral indices for both the 2PL and 3PL fits to each range. The average 3PL transition range fit for the χ_{2PL}^2 population values, $\langle \alpha_T^{\chi_{2PL}^2} \rangle = -3.18$, is significantly close to the mean kinetic range index for the 2PL fit, -2.9 .

The spacecraft frequencies f_{ρ_i} , f_{d_i} and $f_{\rho_{disp}}$ associated with wave-numbers corresponding to the ion gyro-

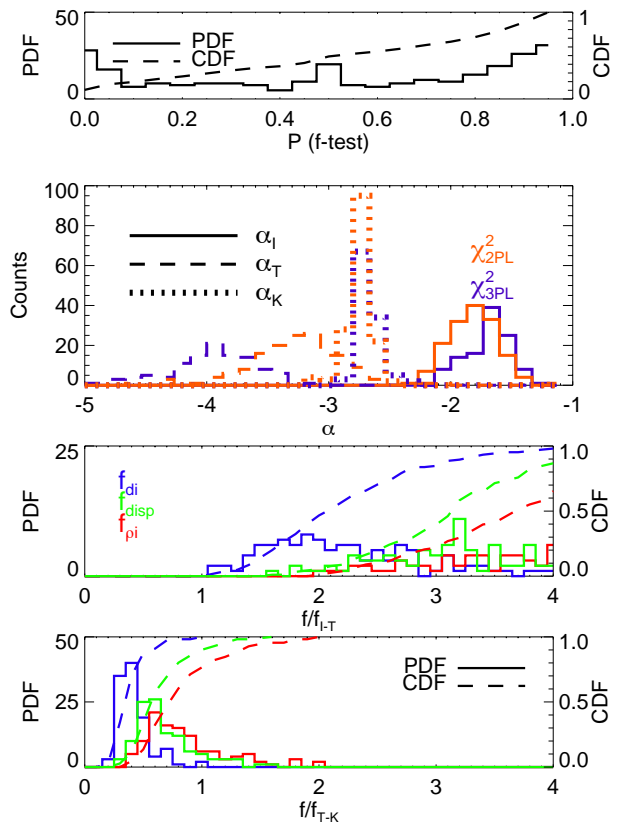


FIG. 2: (a) Histogram of f -test significance values $P(F)$; the cumulative distribution is shown as a dashed line. (b) Distribution of fitted spectral indices for the χ_{3PL}^2 (blue) and χ_{2PL}^2 (orange) populations, in the inertial α_I (solid), transition α_T (dashed), and kinetic α_K (dotted) ranges. (c,d) Measured break frequencies (f_{IT}, f_{TK}) compared to physical plasma scales: f_{ρ} (red), f_{d_i} (blue), and f_{disp} (green).

TABLE I: Measured mean spectral indices from 3PL and 2PL fits to both χ_{2PL}^2 and χ_{3PL}^2 populations.

Pop.	2PL Fit		3PL Fit		
	$\langle \alpha_I \rangle$	$\langle \alpha_K \rangle$	$\langle \alpha_I \rangle$	$\langle \alpha_T \rangle$	$\langle \alpha_K \rangle$
χ_{2PL}^2	-1.7	-2.9	-1.7	-3.1	-2.7
χ_{3PL}^2	-1.6	-3.1	-1.6	-3.9	-2.6

scale ρ_i , inertial scale $d_i = \rho_i / \sqrt{\beta_i}$ and the “dispersion scale” $\rho_{disp} = \rho_i \sqrt{(1 + T_{0c}/T_{0i})/2}$ at which the KAW become dispersive [52], respectively, are computed using the Taylor hypothesis $2\pi f = v_{sw}k$ where $\beta_i = v_{thi}^2/V_A^2$ and the Alfvén speed is $v_A = B_0/\sqrt{n_{0i}m_i\mu_0}$.

Figures 2(c,d) show the probability and cumulative distributions of the break scales of the χ_{3PL}^2 population. The measured breakpoints are normalized to the frequencies f_{ρ_i} , f_{d_i} and $f_{\rho_{disp}}$. Figure 2(c) shows that f_{IT}^* , the break from the inertial range to the anomalously steep transition range, occurs at significantly lower frequencies

than any considered physical scale. Figure 2(d) shows that the break between the transition to kinetic ranges, f_{TK}^* , is most similar to f_{ρ_i} .

Physical interpretation: dissipation.— Eq. 4 implies that the observed steep spectra are associated with either significant dissipation or nonlinear speedup of the cascade in the transition range. First assuming that the steep spectrum is due to dissipation [22, 37, 53–57], i.e. ϵ_{k_\perp} decreases with k_\perp across the transition range. It is necessary to then make an assumption about the baseline variation of $\tilde{\omega}_{k_\perp}$ with k . To this end, we construct from our 3PL fits a synthetic spectrum:

$$E^*(f) = \begin{cases} c_I f^{\alpha_I} & \text{if } f < f_{IT}^* \\ c_T f^{\alpha_K} & \text{if } f > f_{IT}^* \end{cases} \quad (6)$$

This joins the fitted inertial-range spectrum to a synthetic spectrum with the fitted kinetic-range exponent α_k at the inertial-transition break f_{IT}^* [62]. An example of this synthetic spectrum is shown in Figure 3(a). We use E^* to determine $\tilde{\omega}_{k_\perp}^*$ (cf. Eqs. 1-2), assuming that this synthetic spectrum is what would result if $\epsilon_{k_\perp}^*$ were constant. Using this synthetic $\tilde{\omega}_{k_\perp}^*$ and the fitted 3PL spectrum E^{3PL} in Eq. 4 results an estimate of the fractional heating rate in the transition range relative to the synthetic spectrum,

$$1 - \hat{Q}^* = \frac{\epsilon_{f_{TK}^*}}{\epsilon_{f_{IT}^*}} = \left(\frac{E^{3PL}(f_{TK}^*)}{E^*(f_{TK}^*)} \right)^{3/2}. \quad (7)$$

Figure 3(b) shows measured ratios of $\epsilon_{TK}/\epsilon_{IT}$ as a function of transition range spectral index α_T . Thus, transition range spectral indices of $\alpha_T \approx -4$ may be a signature of significant ion-scale heating, corresponding in some cases to $> 90\%$ of the turbulent energy flux.

Physical interpretation: nonlinear effects.— Second, it is possible that the anomalously steep transition range spectrum is due to nonlinear effects which dramatically increase $\tilde{\omega}_{k_\perp}$, and therefore also ω_{nl} (cf. Eqs. 2,4) across this range. Let us now assume that ϵ_{k_\perp} is a constant, and use Eq. 4 to determine for each interval the scaling of $\tilde{\omega}_{k_\perp}$, and therefore ω_{nl} , that matches the measured spectrum. Figure 3(c) shows this for one example interval. In the inertial range, the wave-number scalings are similar to those predicted in MHD turbulence models: between $\omega_{nl} \propto k_\perp^{2/3}$ [12] and $\omega_{nl} \propto k_\perp^{1/2}$ [13]. In the kinetic range, the scaling is again similar to predictions of the KAW turbulence models: between $\omega_{nl} \propto k_\perp^{4/3}$ [20] and $\omega_{nl} \propto k_\perp^{5/3}$ [21]. In contrast, within the transition range, ω_{nl} has a very steep scaling, which therefore may be the signature of some nonlinear process speeding up the cascade. Determining the exact mechanism behind this is beyond the scope of this Letter, though several possibilities include tearing mode physics [29–31], interactions between co-propagating dispersive fluctuations [32], or intermittent coherent structures [27, 33, 34].

The fitted E^{3PL} and synthetic E^* spectra allow an estimate of the increase in non-linear interactions due to transition range steepening, using Eq. 1 and taking ϵ_{k_\perp} constant. Figure 3(d) shows the ratio of $\omega_{nl}^{3PL}/\omega_{nl}^*$ evaluated at f_{TK}^* . Thus, for nonlinear effects to explain the steeper spectra without dissipation, ω_{nl} must anomalously increase by a large factor of $\gtrsim 5$.

Discussion.— We have performed a detailed study of the scaling properties of the turbulent fluctuation spectrum in the inner heliosphere using data from the first PSP encounter. We find that the spectrum is well-modelled by either two or three separate power-law scaling ranges. In common with previous measurements at 1AU, we find that at low frequencies, there is an “inertial range” with a spectral index of around $-5/3$ to $-3/2$ [6, 10, 11], while at high frequencies, there is a “kinetic range” with a spectral index of around -2.7 [16–18]. Between these, there often appears an anomalously steep “transition range”, with a highly variable spectrum with mean spectral index around -4 . When observed, this transition range begins at scales much larger than the characteristic ion-kinetic scales, but ends at scales comparable to the ion gyroradius. Our preliminary analysis has not identified clear correlations between signatures of the transition range and background plasma properties critical in identifying the specific process responsible: e.g. $\delta B/B_0$, $\beta_{i,e}$, T_{0e}/T_{0i} .

We show that this steep transition range corresponds to either significant dissipation of the turbulence into heat, or a dramatic nonlinear speedup of the cascade. We use a synthetic spectrum which has the transition range removed to show that, if dissipation is the dominant effect, the mean transition-range spectral index of -3.9 corresponds to 90% of the turbulent energy flux being dissipated into heat over this range, indicating significant ion-scale heating. One important candidate mechanism which could cause this dissipation is stochastic heating [28]. Alternatively, if nonlinear speedup of the cascade is the dominant effect, we show that this means that the nonlinear frequency (inverse cascade time) of the turbulence must increase by a large factor of $\gtrsim 5$ relative to the case without a transition range. Some possibilities that could cause this effect include reconnection onset and the associated loss of dynamic alignment [29, 31], nonlinear interactions between co-propagating waves [32], or the presence of intermittent coherent structures [27, 33, 34].

Further work is needed to distinguish between these mechanisms. The analysis of this Letter shows that, whichever of these explanations turns out to be correct, in the inner heliosphere the observed steepness of the transition range spectrum has dramatic and important effects on the dynamics of collisionless plasma turbulence.

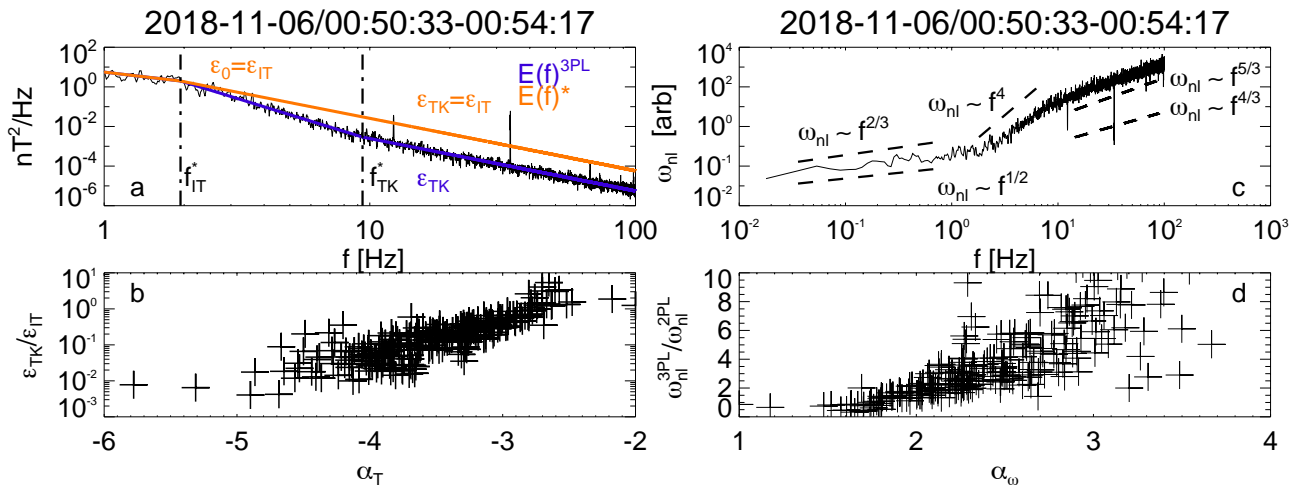


FIG. 3: (a) Measured power spectrum with transition range steepening from Figure 1(a) (black), with the corresponding fitted E^{3PL} (blue) and synthetic E^* (orange) spectra; fitted inertial-transition and transition-kinetic break scales are plotted (vertical dash-dotted lines). (b) Measured ratios of energy flux at transition-kinetic break scale relative to inertial-kinetic scale, $\epsilon_{TK}/\epsilon_{IT}$, plotted against transition range spectral index α_T for all intervals. (c) The dependence of the nonlinear frequency ω_{nl} on spacecraft-frame frequency for interval in (a), assuming constant $\epsilon_{k\perp}$ at all frequencies. Various power-law scalings of $\omega_{nl} \sim f^{\alpha_{nl}}$ are shown with dashed lines. (d) Measured increase of ω_{nl} over the transition range relative to the synthetic spectrum E^* , as a function of the transition range scaling index of the nonlinear frequency, α_ω for all intervals.

* Electronic address: tbowen@berkeley.edu

- [1] John D. Richardson, Karolen I. Paularena, Alan J. Lazarus, and John W. Belcher. Radial evolution of the solar wind from IMP 8 to Voyager 2. *Geophys. Research Letters*, 22(4):325–328, Feb 1995. doi: 10.1029/94GL03273.
- [2] Eliot Quataert. Particle Heating by Alfvénic Turbulence in Hot Accretion Flows. *The Astrophysical Journal*, 500(2):978–991, Jun 1998. doi: 10.1086/305770.
- [3] Steven R. Cranmer. Ion Cyclotron Wave Dissipation in the Solar Corona: The Summed Effect of More than 2000 Ion Species. *The Astrophysical Journal*, 532(2):1197–1208, Apr 2000. doi: 10.1086/308620.
- [4] S. R. Cranmer and A. A. van Ballegoijen. Alfvénic Turbulence in the Extended Solar Corona: Kinetic Effects and Proton Heating. *The Astrophysical Journal*, 594(1):573–591, Sep 2003. doi: 10.1086/376777.
- [5] I. Zhuravleva, E. Churazov, A. A. Schekochihin, S. W. Allen, P. Arévalo, A. C. Fabian, W. R. Forman, J. S. Sanders, A. Simionescu, R. Sunyaev, A. Vikhlinin, and N. Werner. Turbulent heating in galaxy clusters brightest in X-rays. *Nature (London)*, 515(7525):85–87, Nov 2014. doi: 10.1038/nature13830.
- [6] C. H. K. Chen, K. G. Klein, and G. G. Howes. Evidence for electron Landau damping in space plasma turbulence. *Nature Communications*, 10:740, Feb 2019. doi: 10.1038/s41467-019-08435-3.
- [7] T. N. Parashar, C. Salem, R. T. Wicks, H. Karimabadi, S. P. Gary, and W. H. Matthaeus. Turbulent dissipation challenge: a community-driven effort. *Journal of Plasma Physics*, 81(5):905810513, October 2015. doi: 10.1017/S0022377815000860.
- [8] Benjamin D. G. Chandran, Timothy J. Dennis, Eliot Quataert, and Stuart D. Bale. Incorporating Kinetic Physics into a Two-fluid Solar-wind Model with Temperature Anisotropy and Low-frequency Alfvén-wave Turbulence. *The Astrophysical Journal*, 743(2):197, Dec 2011. doi: 10.1088/0004-637X/743/2/197.
- [9] C. H. K. Chen. Recent progress in astrophysical plasma turbulence from solar wind observations. *Journal of Plasma Physics*, 82(6):535820602, Dec 2016. doi: 10.1017/S0022377816001124.
- [10] W. H. Matthaeus and M. L. Goldstein. Measurement of the rugged invariants of magnetohydrodynamic turbulence in the solar wind. *Journal of Geophysical Research*, 87:6011–6028, Aug 1982. doi: 10.1029/JA087iA08p06011.
- [11] J. J. Podesta, D. A. Roberts, and M. L. Goldstein. Spectral Exponents of Kinetic and Magnetic Energy Spectra in Solar Wind Turbulence. *ApJ*, 664:543–548, July 2007. doi: 10.1086/519211.
- [12] P. Goldreich and S. Sridhar. Toward a Theory of Interstellar Turbulence. II. Strong Alfvénic Turbulence. *The Astrophysical Journal*, 438:763, Jan 1995. doi: 10.1086/175121.
- [13] S. Boldyrev. Spectrum of Magnetohydrodynamic Turbulence. *Physical Review Letters*, 96(11):115002, March 2006. doi: 10.1103/PhysRevLett.96.115002.
- [14] B. D. G. Chandran, A. A. Schekochihin, and A. Mallet. Intermittency and Alignment in Strong RMHD Turbulence. *The Astrophysical Journal*, 807(1):39, Jul 2015. doi: 10.1088/0004-637X/807/1/39.
- [15] A. Mallet and A. A. Schekochihin. A statistical model of three-dimensional anisotropy and intermittency in strong Alfvénic turbulence. *MNRAS*, 466(4):3918–3927, Apr 2017. doi: 10.1093/mnras/stw3251.
- [16] O. Alexandrova, V. Carbone, P. Veltri, and L. Sorriso-Valvo. Small-Scale Energy Cascade of the Solar Wind Turbulence. *The Astrophysical Journal*, 674(2):1153–

- 1157, Feb 2008. doi: 10.1086/524056.
- [17] F. Sahaoui, M. L. Goldstein, P. Robert, and Yu. V. Khotyaintsev. Evidence of a Cascade and Dissipation of Solar-Wind Turbulence at the Electron Gyroscale. *Physical Review Letters*, 102(23):231102, Jun 2009. doi: 10.1103/PhysRevLett.102.231102.
- [18] C. H. K. Chen, T. S. Horbury, A. A. Schekochihin, R. T. Wicks, O. Alexandrova, and J. Mitchell. Anisotropy of Solar Wind Turbulence between Ion and Electron Scales. *Physical Review Letters*, 104(25):255002, Jun 2010. doi: 10.1103/PhysRevLett.104.255002.
- [19] CHK Chen, S Boldyrev, Q Xia, and JC Perez. Nature of subproton scale turbulence in the solar wind. *Physical review letters*, 110(22):225002, 2013.
- [20] A. A. Schekochihin, S. C. Cowley, W. Dorland, G. W. Hammett, G. G. Howes, E. Quataert, and T. Tatsuno. Astrophysical Gyrokinetics: Kinetic and Fluid Turbulent Cascades in Magnetized Weakly Collisional Plasmas. *The Astrophysical Journal Supplement*, 182:310–377, May 2009. doi: 10.1088/0067-0049/182/1/310.
- [21] Stanislav Boldyrev and Jean Carlos Perez. Spectrum of Kinetic-Alfvén Turbulence. *ApJ*, 758:L44, Oct 2012. doi: 10.1088/2041-8205/758/2/L44.
- [22] K. U. Denskat, H. J. Beinroth, and F. M. Neubauer. Interplanetary magnetic field power spectra with frequencies from 2.4×10^{-5} Hz to 470 Hz from HELIOS-observations during solarminimum conditions. *Journal of Geophysics Zeitschrift Geophysik*, 54(1):60–67, Jan 1983.
- [23] Robert J. Leamon, Charles W. Smith, Norman F. Ness, William H. Matthaeus, and Hung K. Wong. Observational constraints on the dynamics of the interplanetary magnetic field dissipation range. *Journal of Geophysical Research*, 103(A3):4775–4788, Mar 1998. doi: 10.1029/97JA03394.
- [24] Charles W. Smith, Kathleen Hamilton, Bernard J. Vasquez, and Robert J. Leamon. Dependence of the Dissipation Range Spectrum of Interplanetary Magnetic Fluctuation on the Rate of Energy Cascade. *The Astrophysical Journal Letters*, 645(1):L85–L88, Jul 2006. doi: 10.1086/506151.
- [25] F. Sahaoui, M. L. Goldstein, G. Belmont, P. Canu, and L. Rezeau. Three Dimensional Anisotropic k Spectra of Turbulence at Subproton Scales in the Solar Wind. *Physical Review Letters*, 105(13):131101, Sep 2010. doi: 10.1103/PhysRevLett.105.131101.
- [26] K. H. Kiyani, K. T. Osman, and S. C. Chapman. Dissipation and heating in solar wind turbulence: from the macro to the micro and back again. *Philosophical Transactions of the Royal Society of London Series A*, 373(2041):20140155–20140155, Apr 2015. doi: 10.1098/rsta.2014.0155.
- [27] Sonny Lion, Olga Alexandrova, and Arnaud Zaslavsky. Coherent Events and Spectral Shape at Ion Kinetic Scales in the Fast Solar Wind Turbulence. *The Astrophysical Journal*, 824(1):47, Jun 2016. doi: 10.3847/0004-637X/824/1/47.
- [28] Benjamin D. G. Chandran, Bo Li, Barrett N. Rogers, Eliot Quataert, and Kai Germaschewski. Perpendicular Ion Heating by Low-frequency Alfvén-wave Turbulence in the Solar Wind. *The Astrophysical Journal*, 720(1):503–515, Sep 2010. doi: 10.1088/0004-637X/720/1/503.
- [29] Alfred Mallet, Alexander A. Schekochihin, and Benjamin D. G. Chandran. Disruption of alfvénic turbulence by magnetic reconnection in a collisionless plasma. *Journal of Plasma Physics*, 83(6):905830609, 2017. doi: 10.1017/S0022377817000812.
- [30] Nuno F. Loureiro and Stanislav Boldyrev. Role of Magnetic Reconnection in Magnetohydrodynamic Turbulence. *Physical Review Letters*, 118(24):245101, Jun 2017. doi: 10.1103/PhysRevLett.118.245101.
- [31] Daniel Vech, Alfred Mallet, Kristopher G. Klein, and Justin C. Kasper. Magnetic Reconnection May Control the Ion-scale Spectral Break of Solar Wind Turbulence. *The Astrophysical Journal Letters*, 855(2):L27, Mar 2018. doi: 10.3847/2041-8213/aab351.
- [32] Yuriy Voitenko and Johan De Keyser. MHD-Kinetic Transition in Imbalanced Alfvénic Turbulence. *The Astrophysical Journal Letters*, 832(2):L20, Dec 2016. doi: 10.3847/2041-8205/832/2/L20.
- [33] O Alexandrova. Solar wind vs. magnetosheath turbulence and Alfvén vortices. *Nonlin. Proc. Geophys.*, 15:95, 2008.
- [34] D. Perrone, O. Alexandrova, A. Mangeney, M. Maksimovic, C. Lacombe, V. Rakoto, J. C. Kasper, and D. Jovanovic. Compressive Coherent Structures at Ion Scales in the Slow Solar Wind. *The Astrophysical Journal*, 826(2):196, Aug 2016. doi: 10.3847/0004-637X/826/2/196.
- [35] G. K. Batchelor. *The Theory of Homogeneous Turbulence*. Cambridge University Press, 1953.
- [36] G. G. Howes, S. C. Cowley, W. Dorland, G. W. Hammett, E. Quataert, and A. A. Schekochihin. A model of turbulence in magnetized plasmas: Implications for the dissipation range in the solar wind. *Journal of Geophysical Research (Space Physics)*, 113(A5):A05103, May 2008. doi: 10.1029/2007JA012665.
- [37] G. G. Howes, J. M. Tenbarge, W. Dorland, E. Quataert, A. A. Schekochihin, R. Numata, and T. Tatsuno. Gyrokinetic Simulations of Solar Wind Turbulence from Ion to Electron Scales. *Physical Review Letters*, 107(3):035004, Jul 2011. doi: 10.1103/PhysRevLett.107.035004.
- [38] S. D. Bale, K. Goetz, P. R. Harvey, P. Turin, J. W. Bonnell, T. Dudok de Wit, R. E. Ergun, R. J. MacDowall, M. Pulupa, M. Andre, M. Bolton, J.-L. Bougeret, T. A. Bowen, D. Burgess, C. A. Cattell, B. D. G. Chandran, C. C. Chaston, C. H. K. Chen, M. K. Choi, J. E. Connerney, S. Cranmer, M. Diaz-Aguado, W. Donakowski, J. F. Drake, W. M. Farrell, P. Ferreau, J. Fermin, J. Fischer, N. Fox, D. Glaser, M. Goldstein, D. Gordon, E. Hanson, S. E. Harris, L. M. Hayes, J. J. Hinze, J. V. Hollweg, T. S. Horbury, R. A. Howard, V. Hoxie, G. Jannet, M. Karlsson, J. C. Kasper, P. J. Kellogg, M. Kien, J. A. Klimchuk, V. V. Krasnoselskikh, S. Krucker, J. J. Lynch, M. Maksimovic, D. M. Malaspina, S. Marker, P. Martin, J. Martinez-Oliveros, J. McCauley, D. J. McComas, T. McDonald, N. Meyer-Vernet, M. Moncuquet, S. J. Monson, F. S. Mozer, S. D. Murphy, J. Odom, R. Oliveros, J. Olson, E. N. Parker, D. Pankow, T. Phan, E. Quataert, T. Quinn, S. W. Ruplin, C. Salem, D. Seitz, D. A. Sheppard, A. Siy, K. Stevens, D. Summers, A. Szabo, M. Timofeeva, A. Vaivads, M. Velli, A. Yehle, D. Werthimer, and J. R. Wygant. The FIELDS Instrument Suite for Solar Probe Plus. Measuring the Coronal Plasma and Magnetic Field, Plasma Waves and Turbulence, and Radio Signatures of Solar Transients. *Space Science Rev.*, 204:49–82, December 2016. doi: 10.1007/s11214-016-0244-5.
- [39] Justin C. Kasper, Robert Abiad, Gerry Austin, Marianne Balat-Pichelin, Stuart D. Bale, John W. Belcher, Peter Berg, Henry Bergner, Matthieu Berthomier, Jay Book-

- binder, Etienne Brodu, David Caldwell, Anthony W. Case, Benjamin D. G. Chandran, Peter Cheimets, Jonathan W. Cirtain, Steven R. Cranmer, David W. Curtis, Peter Daigneau, Greg Dalton, Brahmananda Dasgupta, David DeTomaso, Millan Diaz-Aguado, Blagoje Djordjevic, Bill Donaskowski, Michael Effinger, Vladimir Florinski, Nichola Fox, Mark Freeman, Dennis Gallagher, S. Peter Gary, Tom Gauron, Richard Gates, Melvin Goldstein, Leon Golub, Dorothy A. Gordon, Reid Gurnee, Giora Guth, Jasper Halekas, Ken Hatch, Jacob Heerikuisen, George Ho, Qiang Hu, Greg Johnson, Steven P. Jordan, Kelly E. Korreck, Davin Larson, Alan J. Lazarus, Gang Li, Roberto Livi, Michael Ludlam, Milan Maksimovic, James P. McFadden, William Marchant, Bennet A. Maruca, David J. McComas, Luciana Messina, Tony Mercer, Sang Park, Andrew M. Peddie, Nikolai Pogorelov, Matthew J. Reinhart, John D. Richardson, Miles Robinson, Irene Rosen, Ruth M. Skoug, Amanda Slagle, John T. Steinberg, Michael L. Stevens, Adam Szabo, Ellen R. Taylor, Chris Tiu, Paul Turin, Marco Velli, Gary Webb, Phyllis Whittlesey, Ken Wright, S. T. Wu, and Gary Zank. Solar wind electrons alphas and protons (sweep) investigation: Design of the solar wind and coronal plasma instrument suite for solar probe plus. *Space Science Reviews*, 204(1):131–186, Dec 2016. ISSN 1572-9672. doi: 10.1007/s11214-015-0206-3. URL <https://doi.org/10.1007/s11214-015-0206-3>.
- [40] N. J. Fox, M. C. Velli, S. D. Bale, R. Decker, A. Driesman, R. A. Howard, J. C. Kasper, J. Kinnison, M. Kusterer, D. Lario, M. K. Lockwood, D. J. McComas, N. E. Raouafi, and A. Szabo. The solar probe plus mission: Humanity’s first visit to our star. *Space Science Reviews*, 204(1):7–48, Dec 2016. ISSN 1572-9672. doi: 10.1007/s11214-015-0211-6. URL <https://doi.org/10.1007/s11214-015-0211-6>.
- [41] Mihailo M. Martinović, Kristopher G. Klein, Justin C. Kasper, Anthony W. Case, Kelly E. Korreck, Davin Larson, Roberto Livi, Michael Stevens, Phyllis Whittlesey, Benjamin D. G. Chandran, Ben L. Alterman, Jia Huang, Christopher H. K. Chen, Stuart D. Bale, Marc Pulupa, David M. Malaspina, John W. Bonnell, Peter R. Harvey, Keith Goetz, Thierry Dudok de Wit, and Robert J. MacDowall. The Enhancement of Proton Stochastic Heating in the near-Sun Solar Wind. *arXiv e-prints*, art. arXiv:1912.02653, Dec 2019.
- [42] Michael D. McManus, Trevor A. Bowen, Alfred Mallet, Christopher H. K. Chen, Benjamin D. G. Chandran, Stuart D. Bale, Davin E. Larson, Thierry Dudok de Wit, Justin C. Kasper, Michael Stevens, Phyllis Whittlesey, Roberto Livi, Kelly E. Korreck, Keith Goetz, Peter R. Harvey, Marc Pulupa, Robert J. MacDowall, David M. Malaspina, Anthony W. Case, and John W. Bonnell. Cross Helicity Reversals In Magnetic Switchbacks. *arXiv e-prints*, art. arXiv:1912.07823, Dec 2019.
- [43] SD Bale, ST Badman, JW Bonnell, TA Bowen, D Burgess, AW Case, CA Cattell, BDG Chandran, CC Chaston, CHK Chen, et al. Highly structured slow solar wind emerging from an equatorial coronal hole. *Nature*, pages 1–6, 2019.
- [44] Thierry Dudok de Wit, Vladimir V. Krasnoselskikh, Stuart D. Bale, John W. Bonnell, Trevor A. Bowen, Christopher H. K. Chen, Clara Froment, Keith Goetz, Peter R. Harvey, Vamsee Krishna Jagarlamudi, Andrea Larosa, Robert J. MacDowall, David M. Malaspina, William H. Matthaeus, Marc Pulupa, Marco Velli, and Phyllis L. Whittlesey. Switchbacks in the near-Sun magnetic field: long memory and impact on the turbulence cascade. *arXiv e-prints*, art. arXiv:1912.02856, Dec 2019.
- [45] Daniel Vech, Justin C. Kasper, Kristopher G. Klein, Jia Huang, Michael L. Stevens, Christopher H. K. Chen, Anthony W. Case, Kelly Korreck, Stuart D. Bale, Trevor A. Bowen, Phyllis L. Whittlesey, Roberto Livi, Davin E. Larson, David Malaspina, Marc Pulupa, John Bonnell, Peter Harvey, Keith Goetz, Thierry Dudok de Wit, and Robert MacDowall. Kinetic Scale Spectral Features of Cross Helicity and Residual Energy in the Inner Heliosphere. *arXiv e-prints*, art. arXiv:1912.07719, Dec 2019.
- [46] T.A. Bowen, S.D. Bale, T. Bonnell, J.W. and Dudok de Wit, K. Goetz, K. Goodrich, P.R. Gruesbeck J. and Harvey, G. Jannet, A. Koval, R.J. MacDowall, D.M. Malaspina, M. Pulupa, C. Revillet, D. Sheppard, and A. Szabo. A Merged Search-Coil and Fluxgate Magnetometer Data Product for Parker Solar Probe FIELDS. *arXiv e-prints*, art. arXiv, Jan 2020.
- [47] Anthony Case and et al. *ApJS*, 2020.
- [48] Jasper Halekas and et al. *ApJS*, 2020.
- [49] Trevor Bowen, Alfred Mallet, Jia Huang, Kristopher G. Klein, David M. Malaspina, Michael L. Stevens, Stuart D. Bale, John W. Bonnell, Anthony W. Case, Benjamin D. Chandran, Christopher Chaston, Christopher H. Chen, Thierry Dudok de Wit, Keith Goetz, Peter R. Harvey, Gregory G. Howes, Justin C. Kasper, Kelly Korreck, Davin E. Larson, Roberto Livi, Robert J. MacDowall, Michael McManus, Marc Pulupa, J Verniero, and Phyllis Whittlesey. Ion Scale Electromagnetic Waves in the Inner Heliosphere. *arXiv e-prints*, art. arXiv:1912.02361, Dec 2019.
- [50] Gregory G. Howes, Steven C. Cowley, William Dorland, Gregory W. Hammett, Eliot Quataert, and Alexander A. Schekochihin. Astrophysical Gyrokinetics: Basic Equations and Linear Theory. *The Astrophysical Journal*, 651(1):590–614, Nov 2006. doi: 10.1086/506172.
- [51] William H. Press, Saul A. Teukolsky, William T. Vetterling, and Brian P. Flannery. *Numerical Recipes in C (2Nd Ed.): The Art of Scientific Computing*. Cambridge University Press, New York, NY, USA, 1992. ISBN 0-521-43108-5.
- [52] C. A. Kletzing, S. R. Bounds, J. Martin-Hiner, W. Gekelman, and C. Mitchell. Measurements of the Shear Alfvén Wave Dispersion for Finite Perpendicular Wave Number. *Physical Review Letters*, 90(3):035004, Jan 2003. doi: 10.1103/PhysRevLett.90.035004.
- [53] M. L. Goldstein, D. A. Roberts, and C. A. Fitch. Properties of the fluctuating magnetic helicity in the inertial and dissipation ranges of solar wind turbulence. *Journal of Geophysical Research*, 99(A6):11519–11538, Jun 1994. doi: 10.1029/94JA00789.
- [54] Eliot Quataert and Andrei Gruzinov. Turbulence and Particle Heating in Advection-dominated Accretion Flows. *The Astrophysical Journal*, 520(1):248–255, Jul 1999. doi: 10.1086/307423.
- [55] Hui Li, S. Peter Gary, and Olaf Stawicki. On the dissipation of magnetic fluctuations in the solar wind. *Geophys. Research Letters*, 28(7):1347–1350, Apr 2001. doi: 10.1029/2000GL012501.
- [56] T. Passot and P. L. Sulem. A Model for the Non-universal Power Law of the Solar Wind Sub-ion-scale Magnetic Spectrum. *The Astrophysical Journal Letters*, 812(2):

L37, Oct 2015. doi: 10.1088/2041-8205/812/2/L37.

- [57] Anne Schreiner and Joachim Saur. A Model for Dissipation of Solar Wind Magnetic Turbulence by Kinetic Alfvén Waves at Electron Scales: Comparison with Observations. *The Astrophysical Journal*, 835(2):133, Feb 2017. doi: 10.3847/1538-4357/835/2/133.
- [58] We have absorbed all *a priori* unknown constants of order unity into the definitions of ω_{ni} and $\tilde{\omega}_{k_{\perp}}$.
- [59] Two examples of the latter are the following: first, deep in the subion range the linear dispersion of KAW should impose $\tilde{\omega}_{k_{\perp}} \sim k_{\perp} \rho_i$, which steepens the spectrum to the previously mentioned $k_{\perp}^{-7/3}$. Second, incorporating dynamic alignment at large scales [13] provides $\tilde{\omega}_{k_{\perp}} \propto k_{\perp}^{-1/4}$, which gives the expected $k_{\perp}^{-3/2}$ spectrum.
- [60] No significant impact on the results is obtained when the trace magnetic-field spectrum is used without this correction; this is likely because all the relevant quantities scale in the same way with wavenumber.
- [61] the set of all 2PL fits is within the span of 3PL fits
- [62] Another possibility is to extend the inertial-range spectrum up to the transition-kinetic break: as can be seen, this will always result in larger fractional heating rates. We have also neglected the possibility of heating associated with the kinetic range spectral index of around $-8/3$: again, this would increase the overall heating rate. Thus, our procedure gives a lower bound on the heating.